Journal of Chemical Technology and Metallurgy, 50, 2, 2015, 176-182

PREDICTING THE EFFECT OF CELL GEOMETRY AND FLUID VELOCITY ON PEM FUEL CELL PERFORMANCE BY CFD SIMULATION

Bahman ZareNezhad, Mohammad M. Sabzemeidani

Faculty of Chemical, Petroleum and Gas Engineering,
Semnan University, PO Box 35195-363, Semnan, Iran
E-mail: bzarenezhad@semnan.ac.ir

Received 04 November 2014
Accepted 30 January 2015

ABSTRACT

The CFD simulation of a proton exchange membrane (PEM) fuel cell has been carried out to investigate the effects of different parameters influencing cell performance. The model considers the mass and momentum transfer, charge conservation and electrochemical reactions in the presence of membrane and catalyst. The predicted polarization curve is in good agreement with the measured data in the range 0 - 1 A/cm^2. An increase in flow velocity from 0.1 to 0.5 m/s leads to a decrease in the optimum channel width from 0.8 to 0.6 mm. Also there is a sharp decrease in current density as the channel width increases above 0.8 mm at all flow velocities. The presented CFD approach can be used for determination of the optimum fluid velocity and channel geometry of a PEM fuel cell.

Keywords: *PEM fuel cell, CFD simulation, channel width, current density.*

INTRODUCTION

There has been a significant progress in the studies of the proton exchange membrane (PEM) fuel cell technology in the last decade. Despite great successes, the automotive application of PEM fuel cell (PEMFC) faces many technical challenges [1, 2]. A PEM fuel cell consists of three essential compartments: polymer electrolyte membrane, an anode and a cathode [3]. At the anode the hydrogen is oxidized into electrons and protons, while at the cathode, the oxygen is reduced [4]. The wet reactant gas transfers through the gas diffusion layer (GDL) into the catalyst layer where the electrochemical reactions take place [5]. Electrodes are considered as porous media where reactant gases are distributed on the catalyst layers [6]. The PEM fuel cell is a renewable energy source and is important because of factors such as low operating temperatures, modular structure, quick start-up time, high power density, corrosion resistance and environmental benefits. On the other hand, the fuel cells technologies are still more expensive than the conventional fossile fule-based alternatives [7].

The flow field design and scale of a bipolar plate is one of the significant issues in PEM fuel cells [8]. Maharudrayya et al. studied the pressure drop and flow distribution in multiple parallel channel configurations, used in PEM fuel cell stacks [9]. Dutta et al. obtained velocity, density and pressure contours in the gas diffusion layers [10]. They used a finite volume technique for solving model equations. Their results showed that the current direction is drastically dependent on the mass transfer mechanism in the membrane-electrode assembly. Futerko and Hsing applied finite element method (FEM) for solving governing equations in the gas diffusion layers and flow channels [11].They studied the resistance of membranes in polymer electrolyte fuel cells. Their modeling findings illustrated the conclusion that the mole fraction of reactant gases, water content in the membrane and current density are dependent on pressure. More recently, Rodatz et al. carried out studies on the operational aspects of a PEM fuel cell stack under practical conditions [12]. Their work focused exclu-

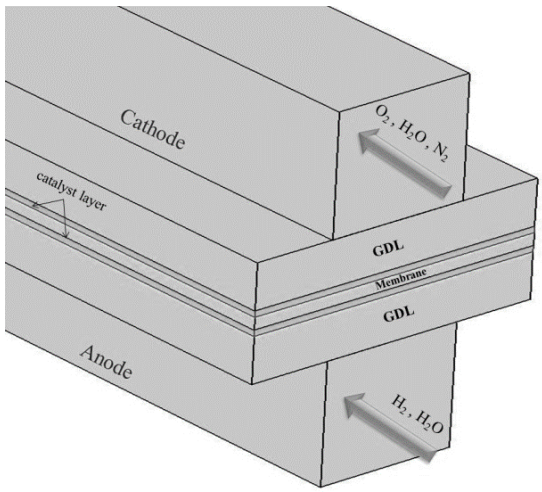

Fig. 1. Schematic diagram of a PEM fuel cell.

sively on the pressure drop, two-phase flow and effect of bends. They noticed a decrease in the pressure drops at a reduced stack current. Ahmed and Sung performed a numerical model to investigate the effects of channel geometrical configuration [13].

In this work, the effects of channel geometry and fluid velocity on the performance of a single PEM fuel cell with a straight channel at co-current flow conditions are evaluated and the optimal operating conditions at different flow conditions are investigated by CFD simulation. The schematic diagram of simulated PEM fuel cell comprising a cathode, an anode, gas diffusion layers , catalyst layers and a proton exchange membrane is shown in Fig. 1.

Proposed CFD Modeling

A 3-dimensional isothermal model is developed to account for the mass, momentum and species balances in the flow channels, GDL and the catalyst layers. Electrochemical reactions in the catalyst layer and GDL parts of the fuel cell and membrane are also considered in the proposed model. Model assumptions include steady state condition, laminar flow regime, ideal gas behavior, gas phase, fixed proton conductivity of membrane, isotropic gas diffusion layer, activation over potential is constant, the membrane is not permeable for reactant gases, isothermal operation. All governing equations are summarized as follows:

Continuity equation:

$$\rho\nabla.\vec{u} = Q_{br} \tag{1}$$

Momentum balance equation:

$$\nabla.[-p+\frac{\mu}{\varepsilon_p}((\nabla\vec{u})+(\nabla\vec{u})^T)-\frac{2\mu}{3\varepsilon_p}(\nabla\vec{u})]-$$

$$-\frac{2\mu}{3\varepsilon_p}(\nabla\vec{u})]-(\frac{\mu}{k_{br}}+\frac{Q_{br}}{\varepsilon_p^{\,2}})\vec{u}=0 \tag{2}$$

Mass transfer equation:

$$\nabla.\vec{j}_i+\rho(\vec{u}.\nabla)\omega_i = R_i \tag{3}$$

Charge conservation equation:

$$\nabla.(\sigma_e^{eff}\nabla\phi_e) = \pm i_{v,total} \tag{4}$$

where Q_{br} is source term in the catalyst layer due to reaction of reactant species and can be calculated from the following equation:

$$Q_{br} = \sum_m\sum_i R_{i,m}M_i \tag{5}$$

$R_{i,m}$ are the electrochemical reactions of hydrogen and oxygen and water:

$$R_{i,m} = \frac{\upsilon_{i,m}i_v}{n_m F} \tag{6}$$

The electrochemical reactions of the sink term for water, hydrogen and oxygen are shown in Table 1.

The diffusional mass flux vector is calculated from the equation:

$$\vec{j}_i = -(\rho\omega_i\sum_k D_{ik}(\nabla x_k+\frac{1}{p_A}[(x_k-\omega_k)\nabla p_A])) \tag{7}$$

where D_{ik} is diffusivity of mixture that can be calculated using Maxwell-Stefan equations. The Maxwell-Stefan diffusion is a model for describing diffusion in multicomponent systems:

$$D_{ik}^{eff} = \varepsilon^{1.5}D_{ik} \tag{8}$$

Table 1. Electrochemical reactions of the sink term for water, hydrogen and oxygen.

H_2O	H_2	O_2
$\frac{i_v}{2F}$	$-\frac{i_v}{2F}$	$-\frac{i_v}{4F}$

Within porous media, electrical conductivity of electrode and membrane are estimated from the modified Brueggemann equation:[14]

$$\sigma_e^{eff} = \sigma_e \times \varepsilon_e^{1.5} \quad (9)$$

The source term, $i_{v,total}$ is given by:

$$i_{v,total} = \sum_m a_v i_{loc} \quad (10)$$

The current densities, i_{loc} are calculated using the Butler-Volmer equation in anode and in cathode.

$$i_a = i_{0,a}\left(\frac{Y_{H_2}}{Y_{H_2}^{ref}}\right)^{0.5}\left(\exp\left(\frac{\alpha_{a,a}F\eta_{act}}{RT}\right) - \exp\left(\frac{-\alpha_{a,c}F\eta_{act}}{RT}\right)\right) \quad (11)$$

$$i_c = i_{0,c}\left(\frac{Y_{O_2}}{Y_{O_2}^{ref}}\right)\left(\exp\left(\frac{\alpha_{c,a}F\eta_{act}}{RT}\right) - \exp\left(\frac{-\alpha_{c,c}F\eta_{act}}{RT}\right)\right) \quad (12)$$

where $i_{0,a}$ $i_{0,a}$ and $i_{0,c}i_{0,c}$ are the exchange current density of the anode and the cathode at a reference temperature (25°C) and pressure (1 atm), respectively. $\alpha_{a,a}$ $\alpha_{a,a}$ and $\alpha_{a,c}\alpha_{a,c}$ are the anodic and the cathodic transfer coefficients for the reaction at the anode. $\alpha_{c,a}$ $\alpha_{c,a}$ and $\alpha_{c,c}\alpha_{c,c}$ are the anodic and the cathodic transfer coefficients for the reaction at the cathode. $Y_{O2}^{ref}Y_{O2}^{ref}$ and $Y_{H2}^{ref}Y_{H2}^{ref}$ are the mass fractions of hydrogen and oxygen at a reference temperature (25 °C) and pressure (1 atm), respectively. The values of the exchange current density and the transfer coefficients are listed from Siegel et al. [15]. R is the universal gas constant (8.314 J mol^{-1} K^{-1}), F is the Faraday constant (C mol^{-1}), and T is the temperature (K). The activation over potential, η is given by:

$$\eta_{act} = \phi_s - \phi_l - E_{eq} \quad (13)$$

The relevant numerical and geometric parameters for this study are shown in Table 2 and Table 3.

RESULTS AND DISCUSSION

The simulation results are compared with experimental data [16] in Fig. 2. The predicted cell potentialls are in excellent agreement with the measured data in the wide current density range of 0 - 1 A/cm^2.

Fig. 3 shows the effect of the channel width on the current density at a constant channel length and different flow velocities. Depending on the flow velocity, there is an optimum channel width for which a maximum current density is obtained. An increase in the flow velocity from 0.1 to 0.5 m/s leads to a decrease in the optimum channel width from 0.8 to 0.6 mm. There is a sharp decrease in

Table 2. Operating conditions of the simulated PEM fuel cell.

Parameters	Value
Inlet anode/cathode temperature (°C)	80
Inlet anode/cathode pressure (atm)	3
Anode/cathode flow velocity (m/s)	2
Relative humidity of inlet gases (%)	100
Mole ratio of O_2/N_2	0.79/0.21
Mass fraction of H_2O (anode)	0.7
Mass fraction of H_2 (anode)	0.3
Mass fraction of H_2O (cathode)	0.14
Mass fraction of O_2 (cathode)	0.2
Mass fraction of N_2 (cathode)	0.66
Inlet O_2 concentration (kmol/m^3)	0.00086
Inlet H_2 concentration (kmol/m^3)	0.04

Table 3. Geometric parameters of the simulated fuel cell.

Description	Value
Channel length, mm	120
Channel width, mm	1.0
Channel depth, mm	1.2
Membrane thickness, mm	0.036
Catalyst layer thickness, mm	0.012
Electrode thickness, mm	0.21

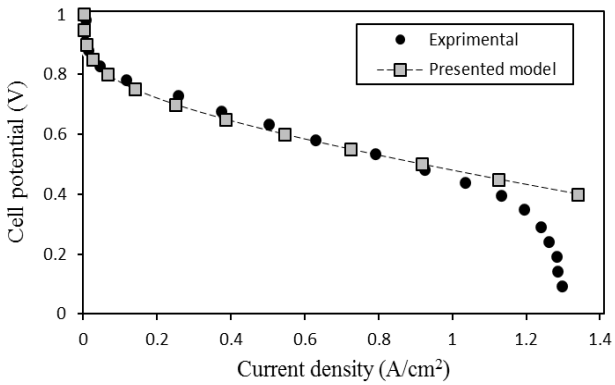

Fig. 2. Comparison between the predicted and the measured cell potential.

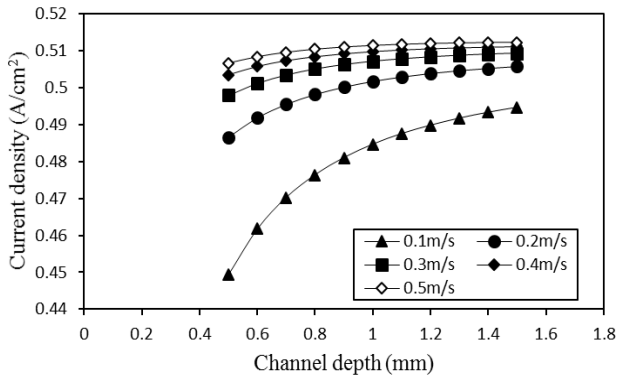

Fig. 4. Effect of channel depth on the PEM fuel cell current density at a cell potential of 0.6V.

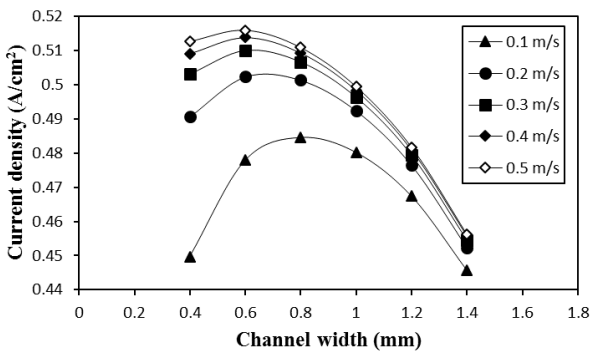

Fig. 3. Effect of channel width on the PEM fuel cell current density at a cell potential of 0.6V.

current density as the channel width increases above 0.8 mm at all flow velocities, shown in Fig. 3.

Fig. 4 shows the effect of channel depth on the current density at a constant channel length and different flow velocities. The numerical results confirm that the current density increases as the channel depth is increased at a constant flow velocity. Comparison of Figs. 3 and 4 suggests that regardless of channel width or depth, there is not a significant change in the current density at flow velocities higher than 0.2 m/s, which is quite interesting from engineering viewpoint.

For a cell potential of 0.6 V, the profile of the hydrogen mole fraction at the anode channel and gas diffusion layer at the different flow velocities, is shown in Fig. 5. This figure testifies that the hydrogen mole fraction at the anode side decreases gradually from inlet to outlet of the channel due to the consumption of hydrogen at the anode catalyst layer. As the mole fraction of hydrogen in the gas diffusion layer decreases, the strong oxidation of hydrogen can be seen. Fig. 5 a,b shows that the

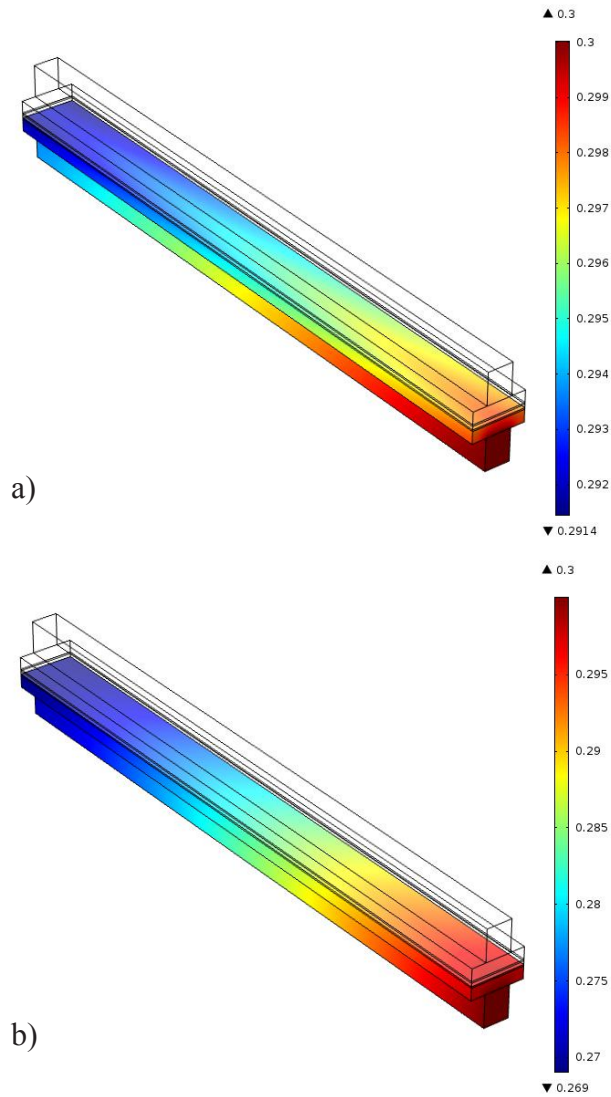

Fig. 5. Hydrogen mole fraction at the anode channel and gas diffusion layer: a) flow velocity 0.1 m/s; b) flow velocity 0.5 m/s.

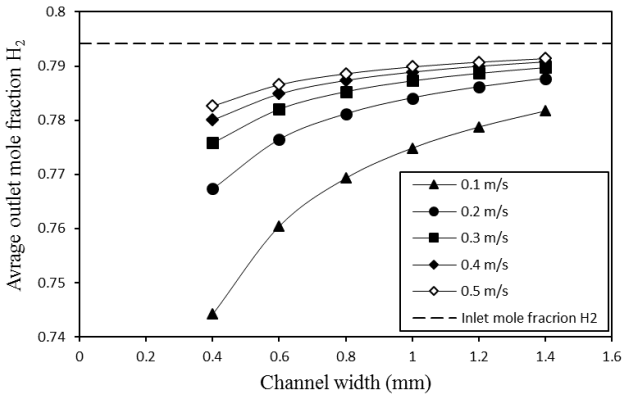

Fig. 6. Effect of channel width on the mole fraction of H_2 at outlet channel.

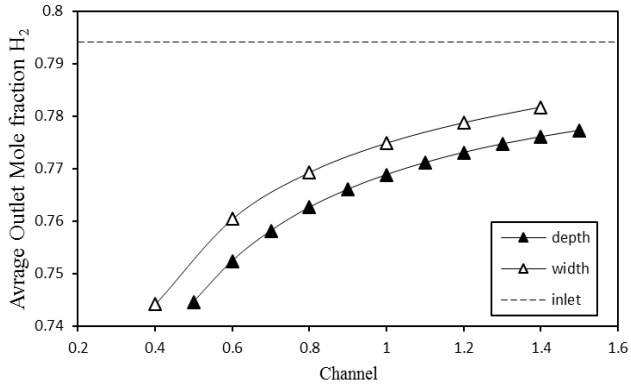

Fig. 8. Effect of channel dimensions on the mole fraction of H_2 at outlet channel.

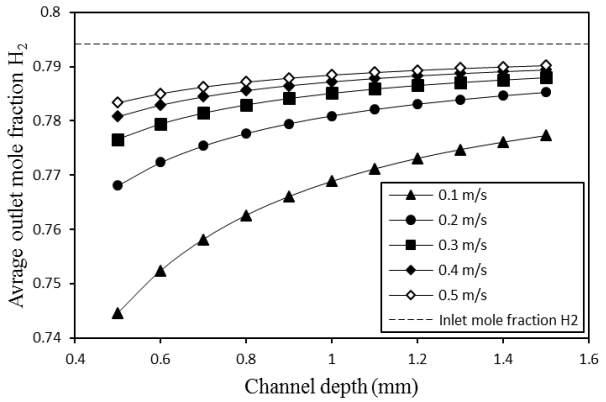

Fig. 7. Effect of channel depth on the mole fraction of H_2 at a outlet channel.

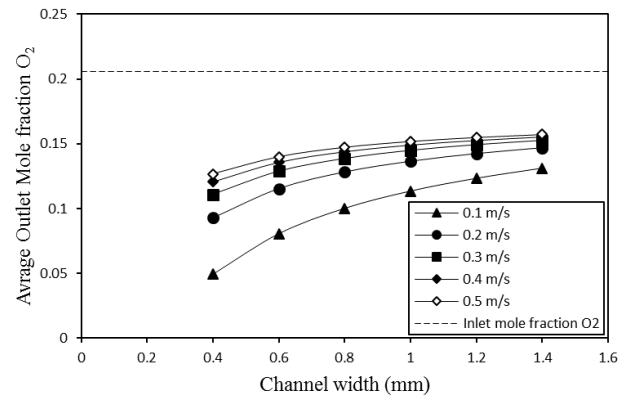

Fig. 9. Effect of channel width on the mole fraction of O_2 at outlet channel.

average outlet mole fraction of H_2 increases, as the flow velocity is increased.

Fig. 6 displays the effect of channel width on the avarage outlet mole fraction of H_2 at a constant channel length for different flow velocities. The predicted results confirm that the avarage outlet mole fraction H_2 is increased, as the channel width is increased at the different flow velocities. As observed, the maximum hydrogen consumption takes place at flow velocity of 0.1 m/s. At flow velocities higher than 0.2 m/s, there is no significant change in the hydrogen mole fraction at the cell outlet.

Fig. 7 displays the effect of channel depth on the avarage outlet mole fraction of H_2 at a constant channel length for different flow velocities. The numerical results confirm that the avrage outlet mole fraction H_2 increases as the channel width is increased at the different flow velocities. As shown, the maximum hydrogen consumption takes place at a flow velocity as low as 0.1 m/s similar to what is observed in Fig. 6.

Fig. 8 compares the effect of channel depth and channel width at a fixed flow velocity of 0.1 m/s. As shown, the channel width is more effective than the channel depth, regarding the mole fraction of hydrogen at the channel outlet.

Fig. 9 displays the effect of channel width on the average outlet mole fraction of O_2 at a constant channel length and a constant channel depth at different flow velocities. The predicted results confirm that the average outlet mole fraction of O_2 increases as the channel width is increased at different flow velocities.

Fig. 10 shows the effect of channel depth on the average outlet mole fraction of O_2 at a constant channel length and a constant channel width, at different flow velocities. The predicted results confirm that the average outlet mole fraction of O_2 increases as the channel depth is increased at the different flow velocities.

Fig. 11 shows the relationship between the average outlet mole fraction of H_2 and the inlet fluid velocity at a cell potential of 0.6 V. It is clearly seen that an

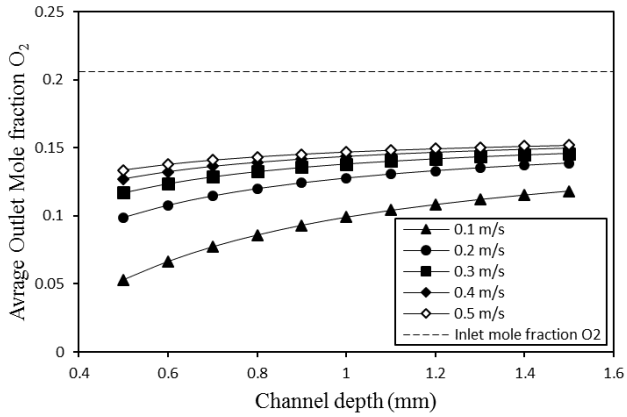

Fig. 10. Effect of channel depth on the mole fraction of O_2 at outlet channel.

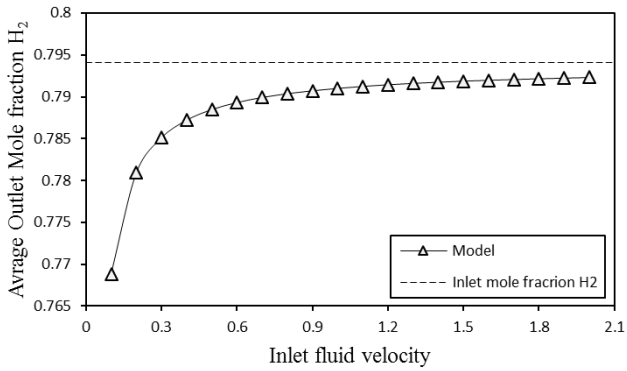

Fig. 11. Effect of inlet fluid velocity on the average outlet mole fraction H_2.

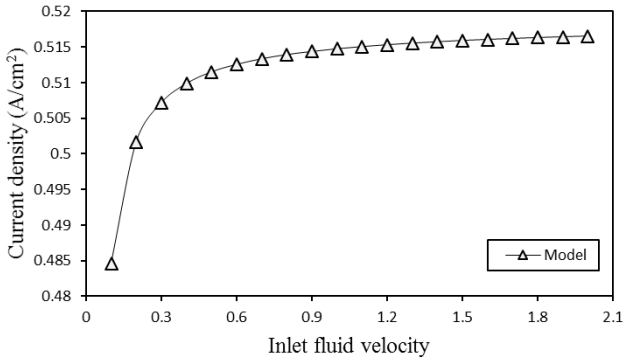

Fig. 12. Effect of inlet fluid velocity on the average current density.

increase in the inlet fluid velocity leads to an increase in the the average outlet mole fraction of H_2. It should be noted that an increase in inlet fluid velocity causes significant hydrogen loss at the channel outlet of PEM fuel cell. The presented CFD approach can be used for determination of the optimum fluid velocity and channel geometry of a PEM fuel cell. As shown in Fig. 12, an increase in flow velocity from 0.1 to 0.5 m/s leads to a considerable increase in the current density. However, an increased flow velocity from 0.1 to 0.5 m/s leads to a significant increase in the mole fraction of H_2 at the cell outlet according to Fig. 11. Therefore, the optimum design of the PEM fuel cell can be established by the proposed CFD model.

CONCLUSIONS

A 3-dimensional CFD simulation of a PEM fuel cell according to a rigorous finite element numerical method is presented. The simulation is conducted to investigate the effect of channel geometry and fluid velocity on the performance of a PEM fuel cell. The predicted polarization curve is in good agreement with the measured data in the range 0 - 1 A/cm^2. An increase in flow velocity from 0.1 to 0.5 m/s leads to a considerable increase in the current density. However, an increased flow velocity from 0.1 to 0.5 m/s leads to a significant increase in the mole fraction of H_2 at the cell outlet. It is found that the channel width is more effective than the channel depth, regarding the mole fraction of hydrogen at the channel outlet. It is shown that depending on the flow velocity, there is an optimum channel width for which a maximum current density is obtained. The optimum design of the PEM fuel cell can be determined by using the proposed CFD model and economic considerations.

REFERENCES

1. S.G. Chalk, J.F. Miller, F.W. Wagner, Challenges for fuel cells in transport applications, J. Power Sources, 86, 2000, 86-94.
2. M.R. Ashraf Khorasani, S. Asghari, A. Mokmeli, M.H. Shahsamandi, B. Faghih Imani, A diagnosis method for identification of the defected cell(s) in the PEM fuel cells, International Journal of Hydrogen Energy, 35, 2010, 9269-9275.
3. J.H. Jang, W.M. Yan, C.C. Shih, Numerical study of reactant gas transport phenomena and cell performance of proton exchange membrane fuel cells, Journal of Power Sources, 156, 2006, 244-252.
4. B. Ramos-Alvarado, A. Hernandez-Guerrero, D. Juarez-Robles, P. Li, Numerical investigation of the performance of symmetric flow distributors as flow channels for PEM fuel cells, International journal of hydrogen energy, 37, 2012, 436-448.

5. H.S Chu, C. Yeh, F. Chen, Effects of porosity change of gas diffuser on performance of proton exchange membrane fuel cell, Journal of Power Sources, 123, 2007, 254-263.
6. F. Hashemi, S. Rowshanzamir, M. Rezakazemi, CFD simulation of PEM fuel cell performance: Effect of straight and serpentine flow fields, Mathematical and Computer Modelling, 55, 2012, 1540-1557.
7. N. Ahmadi, S. Rezazadeh, I. Mirzaee, N. Pourmahmoud, Three-dimensional computational fluid dynamic analysis of the conventional PEM fuel cell and investigation of prominent gas diffusion layers effect, Journal of Mechanical Science and Technology, 26, 2012, 2247-2257.
8. X.D. Wang, Y.Y. Duan, W.M. Yan, Novel serpentine-baffle flow field design for proton exchange membrane fuel cells, Journal of Power Source, 173, 2007, 254-267.
9. S. Maharudrayya, S. Jayanti, A.P. Deshpande, Pressure losses in laminar flow through serpentine channels in fuel cell stacks, J. Power Sources, 138, 2004, 1-13.
10. S. Dutta, S. Shimpalee, J.W. Van Zee, Numerical prediction of mass-exchange between cathode and anode channels in a PEM fuel cell, International Journal of Heat and Mass Transfer, 44, 2001, 2029-2042.
11. P. Futerko, I.M. Hsing, Two-dimensional finite-element method study of the resistance of membranes in polymer electrolyte fuel cells, Electrochimical Acta, 45, 2000, 1741-1751.
12. P. Rodatz, F. Buechi, C. Onder, L. Guzzella, Operational aspects of a large PEFC stack under practical conditions, J. Power Sources, 128, 2004, 208-217.
13. D.H. Ahmed, H.J. Sung, Effects of channel geometrical configuration and shoulder width on PEMFC performance at high current density, J. Power Sources, 162, 2006, 327-339.
14. P.T. Nguyen, T. Berning, N. Djilali, Computational model of a PEM fuel cell with serpentine gas flow channels, J Power Sources, 130, 2004, 149-57.
15. N.P. Siegel, M.W. Ellis, D.J. Nelson, M.R. von Spakovsky, A two-dimensional computational model of a PEMFC with liquid water transport, Journal of Power Sources, 128, 2004, 173-184.
16. L. Wang, A. Husar, T. Zhou, H. Liu, A parametric study of PEM fuel cell performances, International Journal of Hydrogen Energy, 28, 2003, 1263-1272.